Tropical Ecology **58**(4): 717-729, 2017 ISSN 0564-3295

www.tropecol.com

Modelling photosynthetic rates of Indian red mangroves (*Rhizophora mucronata* Poir.) to climatic factors

TANUMI KUMAR[1*], T. V. R. MURTHY[2], PRABAKARAN CHELLAMANI[3], VANITHA KRISHNAN[4], T. THANGARADJOU[4] & R. MANI MURALI[5]

[1]*Regional Remote Sensing Centre-East (RRSC-E), National Remote Sensing Centre (NRSC), Indian Space Research Organisation (ISRO), Kolkata 700 156, India*

[2]*Environment and Hydrology Division (EHD), Space Applications Centre (SAC), Indian Space Research Organisation (ISRO), Ahmedabad 380 015, India*

[3]*Career Point, 343-345, Titanium City Centre Mall, Anandnagar, Ahmedabad 380 015, Gujarat, India*

[4]*Centre of Advanced Study in Marine Biology, Annamalai University, Parangipettai 608 502, Tamil Nadu, India*

[5]*National Institute of Oceanography, Dona Paula, Goa 403 004, India*

Abstract: The paper offers models for simulating photosynthesis as a function of empirical variables, such as radiation, temperature, CO_2 concentrations, water content in the atmosphere, vapour pressure deficit and relative humidity for sun and shade leaves of Indian red mangrove (*Rhizophora mucronata* Poir.). The photosynthetic rates were modelled by incorporating a combination of parameters involved in two separate models, viz. biochemical photosynthetic model and stomatal conductance model together with some additional variables as inputs to two-stage least squares fitting regression method. The results revealed good performance of the models in simulating the photosynthetic rates (in most of the cases validation R^2>0.7 and in some cases as high as 0.92).

Key words: Leaf-level models, simulation, standard error of estimates, validation.

Abbreviations : a – a coefficient; a_i – Initial quantum efficiency; a_{i0} –intrinsic quantum yield of CO_2 assimilation; ANOVA – analysis of variance; BWB – Ball Woodrow Berry; C_i– intercellular CO_2 concentration; CO_2e – carbon dioxide equivalent; CO_2R – reference cell (air) CO_2; CO_2S – sample cell (leaf chamber/ IRGA) CO_2; C_s – CO_2 concentration at the leaf surface; *CTleaf* – computed leaf temperature; g_0 – residual stomatal conductance; g_s – stomatal conductance to water vapour; H_2OR – reference cell H_2O; H_2OS – sample cell H_2O; IRGA – infra-red gas analyzer; L1 – sun leaves; L2 – shade leaves; OLS – ordinary least- squares; PAR_i– in-chamber quantum sensor (*PAR* or PPFD); PAR_o– external quantum sensor (*PAR* or PPFD); *pE* – photosynthetic rate; P_g – gross photosynthetic rate; P_{max} – Maximum photosynthetic rate; P_N – net photosynthetic rate; R – perfect gas constant; R^2 – coefficient of determination; R_d – dark respiration rate; *RH* – relative humidity; *RH_R* – relative humidity in the reference cell; *RH_S* – relative humidity in the sample cell; 2SLS – two-stage least squares regression; SEE – standard error of the estimate; *TBlk* – temperature of the cooler block; *Tr* – rate of transpiration; T_S– temperature in sample cell; V_{max} – maximum catalytic activity of Rubisco per unit leaf area; *VPD* – vapour pressure deficit; *VpdA* – vapour pressure deficit at air temperature; *VpdL* – vapour pressure deficit at leaf temperature; θ – Curvature (reflecting the bending degree of the photosynthetic curve); Γ – CO_2 compensation point.

[*]*Corresponding Author*; e-mail: tanumikumar@yahoo.co.in

Introduction

Mangroves are unique ecosystems – highly productive forests built by a small group of trees and shrubs that have adapted to survive in the harsh interface between land and sea (Spalding *et al.* 2010). More precisely, these forests are the characteristic intertidal plant formations of sheltered tropical and subtropical coastlines (Kathiresan & Bingham 2001). Mangroves are found in 123 countries and territories globally, and cover a total of 152,000 square kilometres (Spalding *et al.* 2010). In recent times, mangrove forests have received much attention due to their vital role in global carbon cycles (Donato *et al.* 2011). The average annual carbon sequestration rate for mangroves has been estimated to be 8 tonnes of carbon dioxide (CO_2) equivalent (CO_2e) ha^{-1} yr^{-1} (Murray *et al.* 2011). Worldwide, there are 114 species of true mangroves belonging to 66 genera (Tomlinson 1994). *Rhizophora mucronata* Poir., belonging to the Rhizophoraceae family, is one such 'red mangrove' species that usually grows in the fringes of tidal mangrove forests. These plants are characterized by 'mucronate' leaves and stilt roots.

Simulation models of physiological processes and assimilation of climatic parameters in those models are of immense significance for the understanding of the impact of climate change on mangroves. There are a number of numerical and empirical simulation models involving various environmental factors with a single physiological process (Barr *et al.* 2009) and several integrated models, where a physiological process has been coupled with stomatal conductance, mass transfer, some biochemical reactions, and energy balance of the leaves of mesophytic plants (Farquhar *et al.* 2001). Though many of these models are useful in the theoretical as well as experimental study of photosynthesis, yet in most of these cases the parameters have been derived from *in-vitro* studies and cannot be readily measured or recorded in the field.

Mangroves grow under extreme environmental and climatic conditions such as high salinity, temperature and radiation (Ball & Critchley 1982; Bjorkmann *et al.* 1988; Moorthy & Kathiresan 1999). Factors affecting photosynthesis in mangroves have been poorly understood. Mwangi *et al.* (2001) investigated the gas exchange properties, water use efficiency and water relations in *R. mucronata* and *Ceriops tagal* at Gazi Bay, Kenya. Again gas exchange and chlorophyll fluorescence have been studied in *R. mucronata* growing under controlled conditions (Ulqodry *et al.* 2014) and in natural conditions at Paklok, Phuket (Wongpattanakul *et al.* 2015); though these works provide information pertaining to the photosynthetic performance, but these do not deal with simulation of photosynthetic rates.

Only a few studies have been carried out on the photosynthetic rate models of mangroves. *In-situ* gas exchange rates of *R. mangle* growing along the shoreline of Key Largo and along the Taylor River in the coastal Florida Everglades were investigated by Barr *et al.* (2009). Mu & Xu (2009) explored the photosynthetic yield of five mangrove species of the mangrove forests of Futian district, Shenzhen. Both the investigations provide models based on one-time measurement of carbon assimilation rate in response to environmental variables; moreover, the authors have neither taken into account the diurnal leaf-level fluxes nor have provided the mathematical expression(s) for the photosynthetic rates. Besides, these works do not discuss about the performance of the models in terms of validation.

In the present endeavour, numerical simulation of photosynthetic rates in *R. mucronata* has been done using *in-situ* diurnal leaf-level measurements. The performances of models have been evaluated in terms of validation. The outcomes can provide better theoretical understanding of the photosynthetic yield in this species. Moreover, the model(s) could be used for simulating the change in the photosynthetic rates of *R. mucronata* in the future climate change perspective. In addition, added knowledge of diurnal leaf-level fluxes and physiological responses to climatic conditions in these mangroves will improve our understanding of carbon fluxes in the concerned ecosystems. Furthermore, the outputs of the present study can also serve as valuable inputs for the up scaling of photosynthesis to the canopy level.

Materials and methods

Study areas

Rhizophora mucronata Poir. growing under natural conditions in the mangrove forests of Chorao (Dr. Salim Ali Bird Sanctuary) and Diwar islands, Goa, lying on the west coast and Pichavaram, Tamil Nadu, lying on the southeast coast of India were used as study stands. The mangrove forests of Chorao and Diwar islands as well as Pichavaram are components of typical estuarine ecosystems (Mandal & Naskar 2008). Pichavaram mangroves receive freshwater mostly

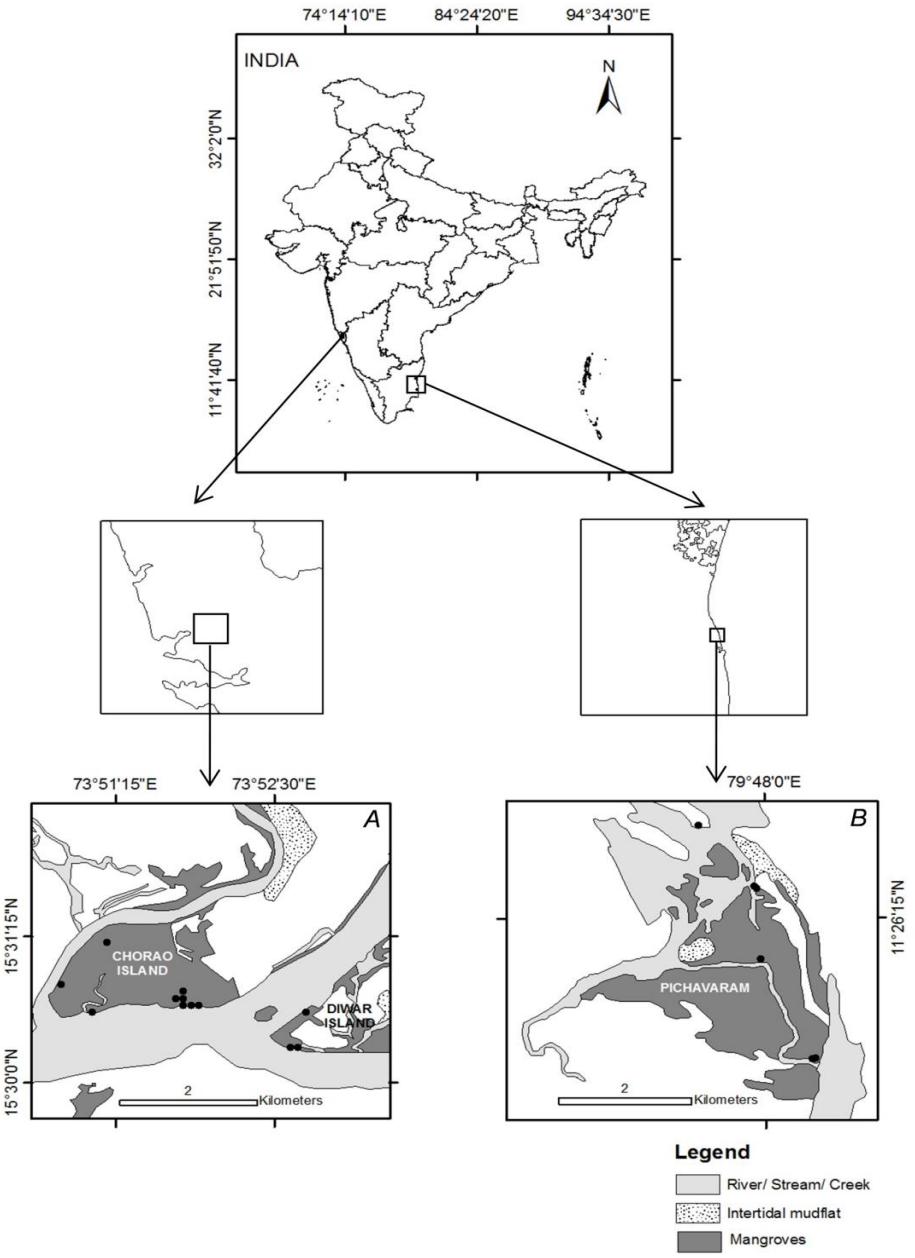

Fig. 1. Locations of the two study areas of mangrove forests in India: (*A*) Chorao and Diwar islands, Goa; (*B*) Pichavaram, Tamil Nadu. Sampling locations depicted in filled black circles. Wetland classes modified after SAC (2009, 2010).

during the northeast monsoon season that extends from October to November. *Rhizophora mucronata* occurs as one of the dominant communities in the two study areas. The sampling locations are shown in Fig. 1.

In-situ measurements

LI-6400XT portable photosynthesis system (Li-cor Co., Ltd., Lincoln, NE, USA) was used for data measurements. The photosynthetic rates of the test/sample trees of *R. mucronata* were measured during the months of April–May (summer season), September–October (post-monsoon period in Goa and period before the northeast monsoons at Tamil Nadu; henceforth in the text this period has been designated as post-monsoon for both the study areas) and December–January (winter season). The method of randomization was used for sampling

and healthy trees were selected and labelled. During cloud-free days of the three seasons measurements were taken for the same selected and labelled trees. The canopy of each test tree was divided into two strata: sun leaves (L1) and shade leaves (L2). Three to five mature green leaves from each stratum were randomly selected based on the condition that leaves were within reach either from land or from boat. Repeated measurements of the leaf photosynthetic rates from before sunlight (from about 06:00 h) till after sunset when photosynthetic rates were observed to be negative (till about 19:00 h were taken with the transparent leaf chamber [infra-red gas analyzer (IRGA) chamber]. Besides photosynthetic rates the portable photosynthesis system also records other physiological and climatic parameters as mentioned in Tables 1S, 2S.

Processing of the collected data

Statistical software, SPSS version 16.0 was used for parameterization and model development. MS Office Excel together with mathematical software Origin Pro 8 was employed in data processing and preparation of graphs.

Basis for model development

Mathematical expression of a physiological or biochemical process may improve our understanding of that process. An empirical model is one whose reliability is based on observations and/or experimental data, which may or may not be supported by any established theory or law. In view of these facts, it may be noted that the relationship of photosynthetic rate and photosynthetically active radiation can be derived based on the already published biochemical model for photosynthesis of C_3 plants (Farquhar *et al.* 1980) as given below:

$$\theta P_g^{\,2} - P_g(a_i \cdot PAR + P_{max}) + a_i \cdot PAR \cdot P_{max} = 0 \qquad (1)$$

The net photosynthetic rate can be represented by a traditional Michaelis-type equation as:

$$P_N = P_g - R_d \qquad (2)$$

Where,

a_i– initial quantum efficiency

P_N– net photosynthetic rate

P_g– gross photosynthetic rate

R_d– dark respiration rate

P_{max}– maximum photosynthetic rate

θ – curvature (reflecting the bending degree of the photosynthetic curve)

The model mainly includes the parameters:

(A) a_i: The initial quantum efficiency is markedly effected by the concentration of intercellular CO_2 (C_i), which can be expressed by the formula:

$$a_i = a_{i0}\,(C_i - \Gamma)/(C_i - 2\Gamma) \qquad (3)$$

Where,

a_{i0}– intrinsic quantum yield of CO_2 assimilation

Γ– CO_2 compensation point. The concentration of CO_2 in the intercellular spaces varies with the outside CO_2 concentration, P_N and stomatal conductance (g_s).

According to Ball Woodrow Berry (BWB) model (Ball *et al.* 1987) under well-hydrated condition of the plant body,

$$g_s = a\frac{P_N \cdot RH}{C_s} + g_0 \qquad (4)$$

Where,

a – a coefficient

RH – relative humidity

C_s – CO_2 concentration at the leaf surface

g_s – stomatal conductance to water vapour

g_0 – residual stomatal conductance

Since stomata respond to humidity deficit rather than to surface relative humidity, the BWB model can be modified by substituting RH with vapour pressure deficit (VPD) (Luening 1995) as given below:

$$g_s = a\frac{P_N}{(C_s - \Gamma)\left(1 - \frac{VPD}{VPD_0}\right)} + g_0 \qquad (5)$$

Where,

P_N approaches zero under diffuse light, g_s also approximates to zero and g_0 is a constant approximate to zero. VPD_0 is an empirically determined coefficient.

When $g_0 = 0$

$$C_i = C_s - a_i(C_s - \Gamma)\left(1 + \frac{VPD}{VPD_0}\right) \qquad (6)$$

Accordingly, the simplified formula shows that C_i primarily depends on the CO_2 concentration in the atmosphere and atmospheric humidity.

(B) *Maximum photosynthetic rate (P_{max})*: This is chiefly controlled by Ribulose-1, 5-bisphosphate carboxylase (Rubisco) and depends on the CO_2 concentration and temperature. The equations are as follows:

$$P_{max} = V_{max}\,(C_s - \Gamma)/(C_i + C) \qquad (7)$$

Where,

V_{max}– maximum catalytic activity of Rubisco per unit leaf area

C – the parameter in the Michaelis' equation of CO_2 and O_2 in Rubisco reaction and is assumed to be a constant here. Since Rubisco is an enzyme, V_{max} depends on temperature (T_a).

$$V_{max} = V_{m0}[1 + \exp\{(-a_1 + b_1 T_a)/RT_a\}]^{-1} \quad (8)$$

Where,

$$V_{m0} = V_0 Q_{10}^{(T_0-25)/10}$$

a_1, b_1 and V_{m0} – parameters

$V_0 = V_{m0}$ at 25 °C

R – perfect gas constant

(C) *Dark respiration rate (R_d)* is proportional to V_m:

$$R_d = kV_m \quad (9)$$

Parameterization of the models

Tables 1S, 2S display the mean values of the *in-situ* measured parameters. The data of L1 and L2 leaves of a test tree were separately subjected to Pearson's correlation analyses (Tables 3S, 4S). Correlation analyses were followed by Two-stage Least Squares Regression (2SLS) fitting method to determine model parameters for L1 and L2 leaves separately. In the 2SLS models (Tables 1, 2), biochemical model for photosynthesis was applied to establish the relationship of photosynthetic rates with air temperature, relative humidity, concentration of water in the air, CO_2 concentration and other parameters which were found to be significantly correlated to the rate of photosynthesis (*pE*), obtained in the outputs of Pearson's correlation analyses (particularly, the reference parameters) (Tables 3S, 4S), i.e. $P_N = f$ (*TS*, *RH_R*, *VpdA*, *CO₂R*, *etc*.). The aforesaid parameters were treated as predictors in the models. The relationship of intercellular CO_2 concentration (C_i) with vapour pressure deficit based on leaf temperature (*VpdL*) and CO_2 concentration on the leaf (C_s or *CO₂R* or *CO₂S*) was formulated on the basis of the stomatal conductance model, i.e. $C_i = f$ (*CO₂S*, *VpdL*, g_s, etc.). Parameters in this conductance model (including C_i) and other factors that were notably associated to C_i (as achieved from the results of correlation analyses) were treated as instrumental variables. Moreover, sunshine (*PAR*) was included as one of the instrumental variables in the models and not as a predictor as in the diurnal pattern of photosynthetic rates in mangroves, role of solar radiation is found to be lesser in comparison to CO_2 concentration, temperature, relative humidity or concentration of water in the air (Ball & Critchley 1982; Kumar *et al.* 2012).

Two-stage Least Squares Regression was implemented because the method is usually helpful when there are feedback loops in the model (Dillon & Goldstein 1984; James & Singh 1978). For example, there is a significant negative correlation between the rate of photosynthesis (*pE*) and C_i (Table 3S, 4S); again, C_i is notably controlled by *CO₂R* and *CO₂S*, so change in these concentrations will not only change C_i, but also alter *pE* values. Moreover, *pE* is also negatively correlated to *CO₂R* and *CO₂S*. Consequently, CO_2 concentration is both a predictor as well as an instrumental variable in the determination of the dependent variable, *pE*. 2SLS regression analysis is a statistical method that is used in the analysis of structural equations. This technique is the extension of the ordinary least-squares (OLS) method. One of the basic assumptions of the OLS regression model is that the values of the error terms are independent of the values of the predictors. When this "recursivity assumption" is broken, the 2SLS model can help solve these problematic predictors. The 2SLS model assumes that there exist instrumental or secondary predictors, which are correlated with the problematic predictors but not with the error term. Given the existence of instrumental variables, the 2SLS model: (1) computes OLS models using the instrumental variables as predictors and the problematic predictors as responses; (2) the model-estimated values from stage 1 are then used in place of the actual values of the problematic predictors to compute an OLS model for the response of interest (Scott & Holt 1982).

Validation of the models

The simulated rates of all sample or test trees were plotted against measured rates to get the coefficient of determination (R^2) values. Validation was carried out for the three seasons and two study areas separately.

Results

Explanation and précis of the models

The model description table gives a synopsis of the model being fit. Factors specified as predictors

Table 1. Model description for sun leaves of *R. mucronata*.

Variable	Abbreviation	Type
Photosynthetic rate	*pE*	dependent
Temperature in sample cell	T_S	predictor & instrumental
Computed leaf temperature	*CTleaf*	predictor
Temperature of the cooler block	*TBlk*	predictor
Reference cell H_2O	H_2OR	predictor & instrumental
Relative humidity in the reference cell	*RH_R*	predictor
Vapour pressure deficit on leaf temperature	*VpdL*	predictor & instrumental
Vapour pressure deficit on air temperature	*VpdA*	predictor & instrumental
Reference cell (air) CO_2	CO_2R	predictor & instrumental
Stomatal conductance	g_s	instrumental
Intercellular CO_2 concentration	C_i	instrumental
External quantum sensor (*PAR* or PPFD)	PAR_O	instrumental
In-chamber quantum sensor (*PAR* or PPFD)	PAR_i	instrumental

Coefficients						Excluded Predictor Variables
	Unstandardized Coefficients					
	B	Standard Error	Beta	t	Significance	
(Constant)	−308.497	60.525		−5.097	0.000	*TBlk*
T_S	19.477	2.077	14.597	9.376	0.000	*VpdA*
CTleaf	−8.153	1.712	−6.000	−4.762	0.000	
H_2OR	−6.487	1.142	−4.302	−5.680	0.000	
RH_R	2.532	0.487	4.758	5.193	0.000	
VpdL	−0.701	3.128	−0.076	−0.224	0.823	
CO_2R	−0.015	0.018	−0.131	−0.828	0.410	

were regressed on the instrumental factors, and the model-estimated values were then used in place of the actual values of these predictors when computing the model for the dependent variable, *pE*. Variables specified as predictors as well as instrumental were used to compute model-estimated values of variables specified as predictors; the actual values of these variables were used when computing the model for *pE*. Again, factors specified as instrumental were used to compute model-estimated values of predictors; these were otherwise not used when computing the model for *pE*. The model parameters for sun and shade leaves are given in Tables 1 and 2, respectively. The multiple correlation coefficient (*R*) was 0.899 for L1 and 0.912 for L2; these values showed linear correlation between the observed and model-predicted values of *pE*. Comparatively higher values signified stronger associations. The squared values of the multiple correlation coefficients (R2 values) depicted that about 80.7% (L1) and 83.2% (L2) of the variations in pE were explained by the individual models. Adjusted R2, an r-squared statistic "corrected" for the intricacy of the models was 0.792 for L1 and 0.819 for L2 and these values were helpful for comparing contending models. Larger values of the statistic indicated improved models. Standard error of the estimate, SEE values (1.291 for L1 and 0.770 for L2) were compared to the standard deviation of pE to see how the models had reduced the uncertainty. Thus, multiple R, R2, adjusted R2 and SEE reported the strength of the relationship between the model and pE. The analysis of variance (ANOVA) tables (Tables 1, 2) tested the acceptability of the models from a statistical perspective. The significance values of the F statistic were <0.05, which meant that the variations that were explained by the models were

Table 2. Model description for shade leaves of *R. mucronata*.

Variable	Abbreviation	Type
Photosynthetic rate	*pE*	dependent
Temperature in sample cell	T_S	predictor& instrumental
Computed leaf temperature	*CTleaf*	predictor
Temperature of the cooler block	*TBlk*	predictor
Reference cell H_2O	H_2OR	predictor
Relative humidity in the reference cell	*RH_R*	predictor& instrumental
Vapour pressure deficit on air temperature	*VpdA*	predictor
Reference cell (air) CO_2	CO_2R	predictor
Intercellular CO_2 concentration	C_i	instrumental
Stomatal conductance	g_s	instrumental
Sample cell (leaf chamber/ IRGA) CO_2	CO_2S	instrumental
Sample cell H_2O	H_2OS	instrumental
External quantum sensor (*PAR* or PPFD)	PAR_O	instrumental
Vapour pressure deficit on leaf temperature	*VpdL*	instrumental

Coefficients						Excluded Predictor Variable
	Unstandardized Coefficients					
	B	Standard Error	Beta	t	Significance	
(Constant)	202.015	51.540		3.920	0.000	*TBlk*
T_S	−0.176	1.990	−0.205	−0.088	0.930	
CTleaf	−9.566	0.589	−10.937	−016.235	0.000	
H_2OR	4.409	1.087	4.594	4.056	0.000	
RH_R	−0.914	0.397	−2.470	−02.301	0.024	
VpdA	28.992	2.674	4.824	10.841	0.000	
CO_2R	−0.016	0.010	−0.219	−01.586	0.117	

not simply due to chance. While the ANOVA were useful tests of the models' ability to explain any variation in *pE*, these did not directly address the strength of the relationships. Tables 1, 2 show the coefficients of the regression lines. Rates of photosynthesis in both L1 and L2 leaves were negatively correlated to C_i and positively correlated to HO_2R and HO_2S (Tables 3S, 4S). The significance values for T_S, *CTleaf*, HO_2R, *RH_R* for L1 leaves (Table 1) and *CTleaf*, *VpdA*, HO_2R for L2 leaves (Table 2) were <0.01, indicating that the effect of these parameters were more distinguishable from the remaining variables in the explanation of the respective predictor, *pE*. The commonly excluded variable in the models was *TBlk*. The common parameters included in the models were CO_2R, H_2OR, *RH_R*, T_S and *CTleaf*. Fig. 2 *A*,*B* shows the diurnal photosynthetic rates of L1 and L2 leaves in the test trees for the parameterization of the respective leaf-level models. The average optimum *pE* for L1 leaves was more than the L2 leaves for all the tree samples irrespective of the study area and season. From Fig. 2*A* it is also evident that optimum *pE* in L1 was achieved before noon.

Verification of the models

The simulation results and the measured values

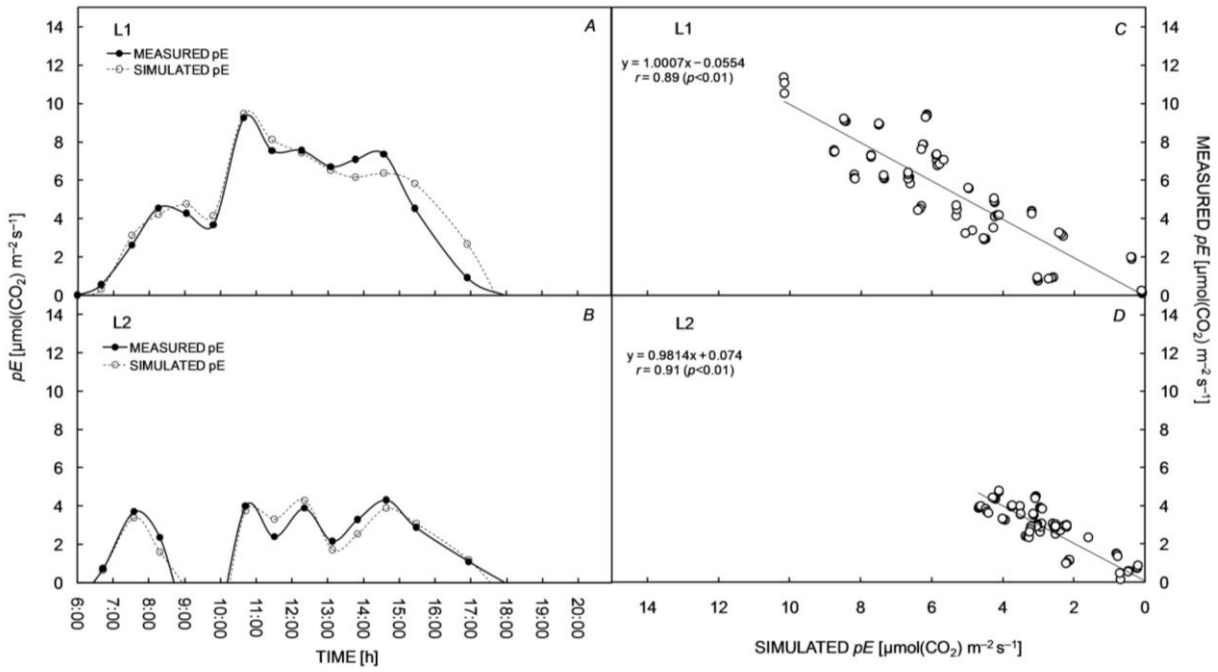

Fig. 2. Graphical representations (*A*, *B*) and correlation analyses of measured photosynthetic rates and those simulated by the models (*C*, *D*) for *R. mucronata* leaves. L1 – sun leaves; L2 – shade leaves; *pE* – photosynthetic rate.

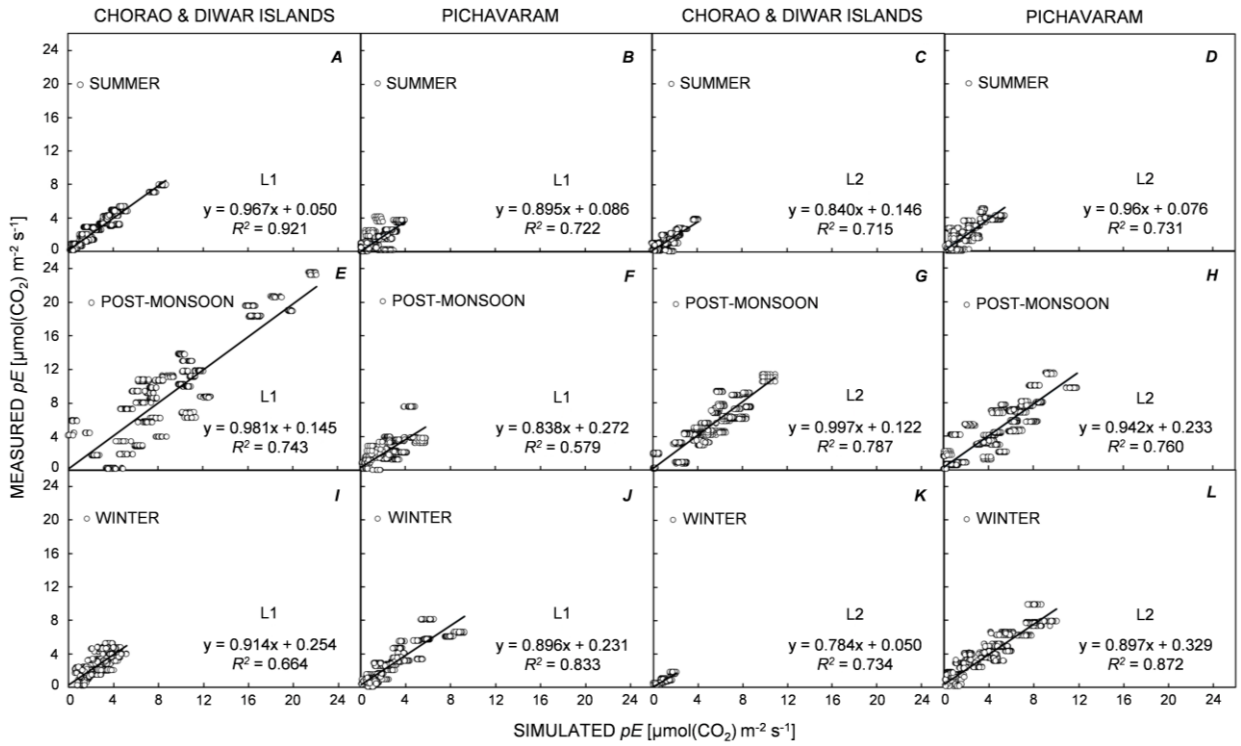

Fig. 3. Validation R^2 at different seasons for L1 and L2 of *R. mucronata* trees at Goa and Pichavaram. L1 – sun leaves; L2 – shade leaves; *pE* – photosynthetic rate.

Table 3. Validation results of the *A. marina* leaf-level models (Kumar *et al.* 2012) on *R. mucronata* leaf samples of the present study. C – constant for linear trend line equation; L1 – sun leaves; L2 – shade leaves; SEE – standard error of the estimate.

Study Area	Season	Layer	*A. marina* model applied on *R. mucronata*		
			R^2	C	SEE
Goa	Summer	L1	0.5949	0.7868	0.8984
		L2	0.6523	0.2202	0.5812
	Post-monsoon	L1	0.7032	0.6787	0.8984
		L2	0.7841	0.1981	0.5812
	Winter	L1	0.4009	0.97	1.1356
		L2	0.6942	0.1063	0.3992
Pichavaram	Summer	L1	0.7021	0.1092	0.7954
		L2	0.3483	0.9647	1.79
	Post-monsoon	L1	0.575	0.2095	1.255
		L2	0.367	1.3608	2.1437
	Winter	L1	0.7994	0.341	1.1448
		L2	0.8971	0.1744	0.9165

had similar trends (Fig. 2 *A*,*B*). Fig. 2 *C*,*D* shows the correlation analyses of measured photosynthetic rates and those simulated by the two models for *R. mucronata* leaves. The slope of the line in both the cases was close to one and the intercept was also near to zero with a significant level ($P < 0.01$). The results indicated a good performance of the models in the simulation of the photosynthetic rates of L1 and L2 leaves.

Validation of the models

Graphical representations of validation R^2 and the validation SEEs for all the samples are given in Fig. 3 and Fig. 4, respectively. For L1 leaves, highest R^2 value (0.921) was noted during summer season at Goa (Fig. 3*A*) and lowest (0.579) during post-monsoon at Pichavaram (Fig. 3*F*); the highest and lowest photosynthetic rates were observed during post-monsoon at Goa and during summer at Pichavaram, respectively (Fig. 3*E*,*B*). For L2 leaves, highest R^2 value (0.872) was computed during winter at Pichavaram (Fig. 3*L*) and lowest (0.715) during summer at Goa (Fig. 3*C*); highest and lowest photosynthetic rates were computed during post monsoon at Pichavaram and winter at Goa, respectively (Fig. 3*H*,*K*). SEE ranged from 0.69–1.12 and 0.3–1.32 µmol CO_2 m^{-2} s^{-1} for L1 leaves at Pichavaram and Goa, respectively (Fig. 4). For L2 leaves SEE ranged from 0.86–1.07 and 0.25–0.8 µmol CO_2 m^{-2} s^{-1} at Pichavaram and Goa, correspondingly (Fig. 4).

Discussion

Models for simulating leaf photosynthetic rates were developed separately for sun and shade leaves. The two types of leaves were dealt separately to demonstrate that there is difference in the variables involved in the regression equation for the respective photosynthetic rates. Air temperature showed higher significance in sun leaves than the shade leaves (Tables 1, 2). It is evident from the results that the simulation precisions of the models were statistically agreeable.

The responses of climatic factors to photosynthesis vary to certain degree, and as a result one needs to focus on the dominant climatic variables and processes. For instance, the solar radiation/*PAR* generally varies from zero to above the light saturation point in a single day, and it is the dominant factor for the daily variations of photosynthesis under the conditions of non severe water stress. Nevertheless, in the photosynthetic models of the current study, *PAR* was considered as an instrumental variable and not as a predictor. Moreover, Ball & Critchley (1982) showed that light saturation level in *Avicennia* studies did not depend on the irradiance of the growth environment under field conditions. Photosynthesis saturated at a much higher *PAR* for L1 leaves than in the L2 leaves (Tables 1S, 2S; Fig. 2 *A*,*B*). Similar observations were reported by Kumar *et al.* (2012) in sun and shade leaves of *Avicennia marina*. The observations are also in accordance with the findings of Ulqodry *et al.* (2014) in which *R. mucronata* seedlings grown under seasonally full light and 50% shade conditions exhibited higher photosynthetic rates than seedlings grown under 80% shade conditions.

Three models of leaf photosynthesis simulation were introduced by Hari *et al.* (1986). The correlation coefficients of the simulated values and the measured data were different under different environmental conditions and it was unfeasible to rank theses models. In the present investigation, the photo response model of photosynthesis (expression 1) was used as the fundamental model, and the effects of other variables were considered as the impact of several factors on the basic model. Moreover, the effect of wind and resistance at the boundary layers of leaf blades were ignored in this study because the wind speed in the IRGA of the

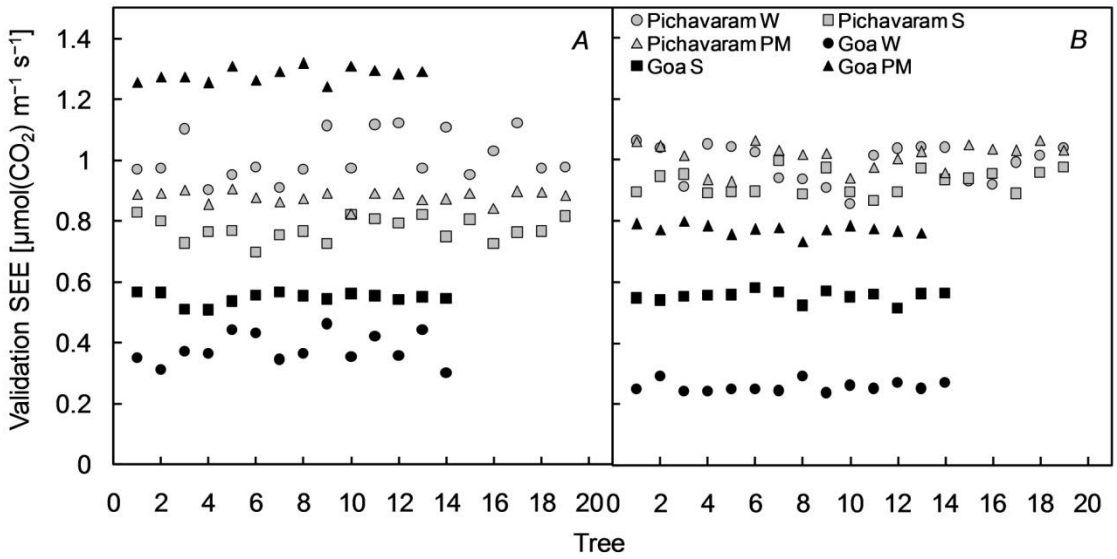

Fig. 4. Validation standard error of the estimates in *R. mucronata* L1 *(A)* and L2 *(B)* at different seasons and study areas. L1 – sun leaves; L2 – shade leaves; PM – post-monsoon; S – summer; SEE – standard error of the estimate; W – winter.

instrument during the measurements was constant so was the resistance at the boundary layers. Again, stomata respond to atmospheric humidity through evaporation from the leaf, rather than to humidity deficit itself (Mott & Parkhurst 1991). Due to a close link between rate of transpiration and vapour pressure deficit on leaf temperature (*VpdL*) [as also revealed in the results of correlation analyses (Tables 3S, 4S)], *VpdL* was preferred in place of transpiration in the stomatal conductance models. This avoided the need to include transpiration in the models for both L1 and L2 leaves (Tables 1, 2).

Kumar *et al.* (2012) provided unique *A. marina* models for sun and shade leaves; these models when validated for the sample trees of *R. mucronata* of the present study, for many of the samples, R square value was either <0.5 or the regression line (trend line) was quite shifted from the origin or the validation SEE was >1.5 (Table 3). Therefore, in the present work, separate leaf-level models were developed for *R. mucronata*. The results showed good performance of the models in simulating the photosynthetic rates (in most of the cases validation R^2>0.7 and in some cases R^2 as high as 0.92).

Overall, the maximum rate of photosynthesis in *R. mucronata* was <10 µmol (CO_2) $m^{-2}s^{-1}$. Such low carbon assimilation rates (an average rate of 4.04 µmol (CO_2) m^{-2} s^{-1} during the wet season) were also reported by Mwangi (1995) for *R. mucronata* trees growing naturally at Gazi Bay, Kenya. As suggested by Smith *et al.* (1989), the reason for reduced carbon assimilation rates may be due in part to the high soil salinities [mean soil salinities of the sampling locations were 24.73 and 21.51 ppt at Tamil Nadu and Goa, respectively (Kumar *et al.* 2015)] which may cause a higher osmotic xylem potential and reduced stomatal conductance. Barr *et al.* (2009) also reported low carbon assimilation rates <4 µmol (CO_2) $m^{-2}s^{-1}$ in the red mangroves of Florida Everglades and attributed hypersaline summer conditions associated with lower xylem water potential as the main causes for such low photosynthetic rates.

The gradual decrease in photosynthetic rates beyond the periods for maximum photosynthesis in case of sun leaves (Fig. 2*A*) may reflect the down-regulation of Rubisco during stomatal closure, perhaps associated with development of water stress and higher leaf temperatures (Cheeseman & Lovelock 2004); higher leaf temperatures were also revealed in the present study (*CTleaf* values for time periods corresponding to the decrease in *pE* values beyond maximum *pE* exceeded 32 °C]. The significant negative correlation between C_i with *pE* (Tables 3S, 4S) seemingly indicated that higher CO_2 concentration could increase the substrate carboxylated by Ribulose-1.5-bisphosphate (RuBP) and reduce the competitive oxidation of O_2 for RuBP and raise the photosynthetic rates of leaves.

The data of more than ten hours were used in the models as the climatic factors (and the photo-synthetic rates) vary greatly in a single day. As

evident from the Tables 1, 2 temperature parameter(s) (particularly *CTleaf*) and water content parameters of the atmosphere played imperative roles in controlling the rates of photosynthesis. Mu & Xu (2009) provided photosynthetic yield model for five mangrove species, but in the model the diurnal variation in the environmental parameters was neglected. Moreover, leaf temperatures and water contents were not explicitly represented in the model. Our data showed that on an average leaf temperature in L1 and L2 leaves increased more than 0.5 °C above air temperature when evaporative cooling decreased with g_s under high irradiance. Stomatal conductance was quite low in *R. mucronata* (an average of 0.05 mol (H_2O) $m^{-2}s^{-1}$) in comparison to *A. marina stomatal* conductance [average value of 0.15 mol (H_2O) $m^{-2}s^{-1}$ (Kumar *et al.* 2015)]. Leaf temperature was also included in the models for *pE*. As evident from Tables 1, 2, water content parameters of the atmosphere played a crucial role in controlling the rates of photosynthesis. Differences in the simulated and measured *pE* values reveal the roles of other factors (which do not appear in the models) influencing the photosynthetic rates.

The present endeavour establishes that the two-stage least squares fitting regression method can be conveniently used for modelling the photosynthetic rates of Indian *R. mucronata* leaves. In the future, these models can be used as sub-models within more complex models for predicting growth of this species. Moreover, the models can also be scaled up from leaf to a canopy of a single tree and finally per unit area of the forests (comprising pure and dominant communities of *R. mucronata*) for the simulation of the interaction between photosynthesis and climatic factors. The field measurements can also be used for estimating light use efficiency in this species.

Acknowledgements

The work was accomplished under the Technology Development/Research and Development (TDP/R&D) Programme (Applications, code: A025) of Space Applications Centre, funded by Department of Space, India. The authors express their sincere gratitude to the respective Principal Chief Conservators of Forests and other forest personnel for granting permissions to take measurements in the forests and the field assistants for their field support. The authors also acknowledge Shri Tanvir-Demetriades Shah (Senior Applications Scientist, Li-cor Biosciences, USA) and Shri Arvind Kumar (Service Engineer, Elron Instrument Company Pvt. Ltd., India) for their valuable inputs on the technicalities of the portable photosynthetic systems. The authors are grateful to the anonymous reviewers for their helpful comments.

References

Ball, J. T., L. E. Woodrow & Berry J. A. 1987. A model predicting stomatal conductance and its contribution to the control of photosynthesis under different environmental conditions. pp. 221–224. *In*: J. Biggens (ed.) *Progress in Photosynthesis Research*, Vol 22. Martinus Nijhof Publishers, The Netherlands.

Ball, M. C. & C. Critchley 1982. Photosynthetic responses to irradiance by the grey mangrove, *Avicennia marina*, grown under different light regimes. *Plant Physiology* **70**: 1101–1106.

Barr, J. G., J. D. Fuentes, V. Engel & J. C. Zieman. 2009. Physiological responses of red mangroves to the climate in the Florida Everglades. *Journal of Geophysical Research.* doi:10.1029/2008JG000843.

Bjorkmann, I., B. Demming & J. T. Andrews. 1988. Mangrove photosynthesis: Response to high irradiance stress. *Australian Journal of Plant Physiology* **15**: 43–61.

Cheeseman, J. M. & C. E. Lovelock. 2004. Photosynthetic characteristics of dwarf and fringe *Rhizophora mangle* L. in a Belizean mangrove. *Plant, Cell and Environment* **27**: 769–780.

Dillon, W. R. & M. Goldstein. 1984. *Multivariate Analysis: Methods and Applications*. Wiley, New York, Chichester, Toronto, Brisbane, Singapore.

Donato, D. C., J. B. Kauffman, D. Murdiyarso, S. Kurnianto, M. Stidham & M. Kanninen. 2011. Mangroves among the most carbon-rich forests in the tropics. *Nature Geoscience* **4**: 293–297.

Farquhar, G.D., S. von Caemmerer & J. A.Berry. 1980. A biochemical model of photosynthetic CO_2 assimilation in leaves of C3 species. *Planta* **149**: 78–90.

Farquhar, G. D., S. von Caemmerer & J. A. Berry. 2001. Models of photosynthesis. *Plant Physiology* **125**: 42–45.

Hari, P., A. Makela, E. Korpilahti & M. Holmberg. 1986. Optimal control of gas exchange. *Tree Physiology* **2**: 169–175.

James, L. R. & B. K. Singh. 1978. An introduction to the logic, assumptions, and basic analytical procedures of two-stage least squares. *Psychological Bulletin* **85**: 1104–1122.

Kathiresan, K. & B. L. Bingham. 2001. Biology of mangroves and mangrove ecosystems. *Advances in Marine Biology* **40**: 81–251.

Kumar, T., T. V. R. Murthy, K. R. Manjunath & C. Prabakaran. 2015. *Modeling PhotosyntheticYield Response of Mangrove Flora to Climatic Factors*. Scientific Report. Space Applications Centre, Ahmedabad, Gujarat, India.

Kumar, T., S. Panigrahy, K. R. Manjunath & C. P. Singh. 2012. Photosynthetic rate model in response to environmental parameters for *Avicennia marina* (Forssk.) Veih. in an Indian mangrove forest. *Acta Physiologiae Plantarum* **34**: 1551–1563.

Luening, R. A. 1995. A critical appraisal of a combined stomatal-photosynthesis model for C_3 plants. *Plant, Cell and Environment* **18**: 339–355.

Mandal, R. N. & K. R. Naskar. 2008. Diversity and classification of Indian mangroves: a review. *Tropical Ecology* **49**: 131–146.

Moorthy, P. & K. Kathiresan.1999. Photosynthetic efficiency in rhizophoracean mangroves with reference to compartmentalization of photosynthetic pigments. *Revista de Biologia Tropical* **47**: 21–25.

Mott, K. A. & D. F. Parkhurst. 1991. Stomatal responses to humidity in air and helox. *Plant, Cell and Environment* **14**: 509–515.

Mu, D. G. & H. L. Xu. 2009. Photosynthetic yield model and the response to environmental factors for five mangrove species. *In*: *Proceedings of the 3rd International Conference on Bioinformatics and Biomedical Engineering*. Institute of Electrical and Electronics Engineers, Beijing, China.doi: 10.1109/ ICBBE.2009.5163189.

Murray, B., L. Pendleton L, W. A. Jenkins & S. Sifleet. 2011. *Green Payments for Blue Carbon: Economic Incentives for Protecting Threatened Coastal Habitats*. Report. Nicholas Institute for Environmental Policy Solutions, NI.

Mwangi, P. M. 1995. *Photosynthesis and Related Processes of Two Mangrove Species: Rhizophora mucronata and Ceriopstagal at Gazi Bay, Kenya*. Ph.D. thesis. University of Nairobi, Kenya.

Mwangi, T., J. Kinyamario & D. V. Speybroeck. 2001. *Rhizophora mucronata* and *Ceriops tagal*, at Gazi Bay, Kenya. *African Journal of Ecology* **37**: 180–193.

SAC. 2009. *National Wetland Atlas: Goa*. Atlas. Space Applications Centre, Ahmedabad, Gujarat, India.

SAC. 2010. *National Wetland Atlas: Tamil Nadu*. Atlas. Space Applications Centre, Ahmedabad, Gujarat, India.

Scott, A. J. & D. Holt. 1982. The effect of two-stage sampling on ordinary least squares methods. *Journal of the American Statistical Association* **77**: 848–854.

Smith, J. A. C., M. Popp, U. Lüttge, W. J. Cram, M. Diaz, H. Griffiths H, H. S. J. Lee *et al*. 1989. Ecophysiology of xerophytic and halophytic vegetation of a coastal alluvial plain in northern Venezuela. VI. Water relations and gas exchange of mangroves. *New Phytologist* **111**: 293–307.

Spalding, M. D., K. Kainuma & L. Collins. 2010. *World Atlas of Mangroves*. A collaborative project of ITTO, ISME, FAO, UNEP-WCMC, UNESCO-MAB, UNU-INWEH and TNC. Earthscan, London.

Tomlinson, P. B. 1994. *The Botany of Mangroves*. Cambridge University Press, New York.

Ulqodry, T. Z., F. Matsumoto, Y. Okimoto, A. Nose & S. H. Zheng. 2014. Study on photosynthetic responses and chlorophyll fluorescence in *Rhizophora mucronata* seedlings under shade regimes fixation capacity. *Acta Physiologiae Plantarum* **36**: 1903–1917.

Wongpattanakul, P., R. J. Ritchie, W. Koedsin & C. Suwanprasit. 2015. Photosynthetic rates in mangroves. pp: 57-61. *In*: *International Conference on Plant, Marine and Environmental Sciences (PMES-2015)*. International Institute of Chemical, Biological and Environmental Engineering, Kuala Lumpur, Malaysia. http://iicbe.org/upload/3865C 0115015.pdf (accessed 10 June 2016).

(Received on 08.09.2016 and accepted after revisions, on 12.02.2018)

Supporting Information

Additional Supporting information may be found in the online version of this article.

Table 1S. Mean values (with ± SE values of the population means within parenthesis) of the *in-situ* measured parameters for *R. mucronata* sun leaves.

Table 2S. Mean values (with ± SE values of the population means within parenthesis) of the *in-situ* measured parameters for *R. mucronata* shade leaves.

Table 3S. Pearson's correlation coefficients amongst *pE* and different parameters for sun leaves of *R. mucronata*.

Table 4S. Pearson's correlation coefficients amongst *pE* and different parameters for shade leaves of *R. mucronata*.